Surface Structural and Chemical Evolution of Layered $LiNi_{0.8}Co_{0.15}Al_{0.05}O_2$ (NCA) Under High Voltage and Elevated Temperature Conditions

Pinaki Mukherjee[1], Nicholas V. Faenza[2], Nathalie Pereira[2], Jim Ciston[3], Louis F. J. Piper[4], Glenn G. Amatucci[2], and Frederic Cosandey[1]

[1] Materials Science and Engineering, Rutgers University, Piscataway, NJ 08854.

[2] Energy Storage Research Group, Department of Materials Science and Engineering, Rutgers University, North Brunswick, NJ 08902, USA.

[3] National Center for Electron Microscopy, Lawrence Berkeley National Laboratory, Berkeley, CA 94720, USA.

[4] Materials Science and Engineering, Binghamton University, Binghamton, NY 13902, USA.

E-mail: grad.pinaki@gmail.com; cosandey@rutgers.edu

*Now at Michigan Technological University, 1400 Townsend Drive, Houghton, MI-49931.

	Rocksalt				Layered	
	Average	Standard Deviation	% Error	Average	Standard Deviation	% Error
Pre/Main	0.42	0.01	3.1	0.41	0.02	4.8
ΔE	11.83	0.05	0.4	12.03	0.70	5.9
Ni- L3/L2	1.61	0.06	3.5	1.71	0.14	8.6
Co- L3/L2	1.54	0.07	4.6	1.52	0.09	6.0
At. % O	67.83	2.08	3.1	70.53	2.01	2.9
At. % Ni	23.08	0.45	2.0	21.85	0.95	4.1
At. % Co	9.09	1.62	17.9	7.62	1.44	19.6
Li-K/Ni-M	1.03	0.10	9.6	0.81	0.13	16.20

Table S1: Statistical analysis of EELS measurements from the area with rocksalt and layered contrast. For each measurement, the average values of raw EELS data are presented along with standard deviation and percentage error. The percentage error is measured as: PE= (Standard deviation/Mean) X 100. For statistical analysis, data from 8-10 nm from the edge have been used. The largest error over 15% occurs for Co concentration and Li-K/Ni-M ratio determinations due to the low EELS signal and inaccuracy in background determination.

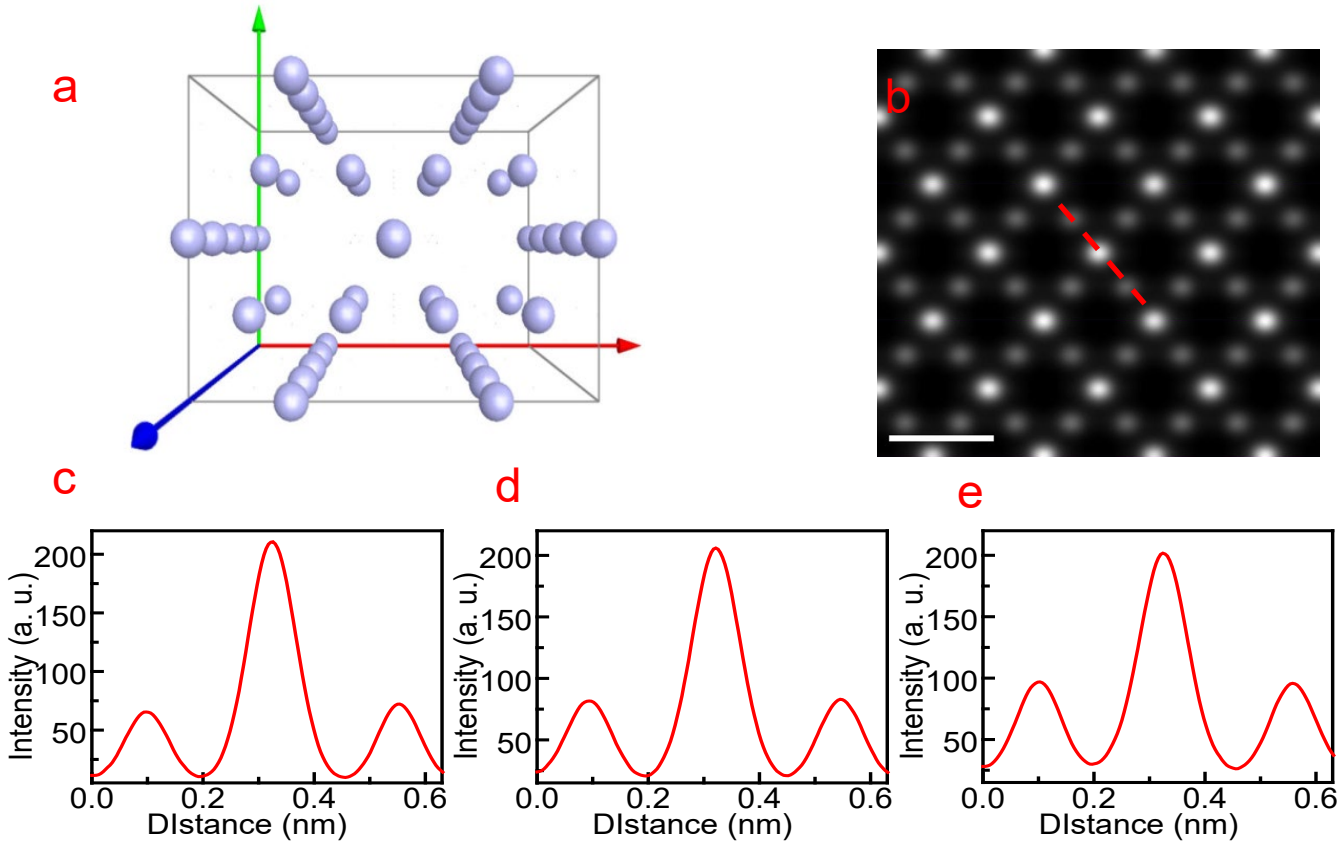

Figure S1: (a) Schematic representation of a supercell of $LiNi_2O_4$ spinel structure viewed along the [110] direction revealing Ni atomic columns containing 0, 2 and 4 Ni atoms in various columns. (Only the Ni atoms are shown here). (b) Multislice simulated HAADF-STEM image of spinel viewed along the [110] zone axis using the frozen lattice formalism with 10 phonon configurations. Experimental conditions correspond to the FEI Titan operated at 300kV with 50 and 200 mrad for inner and outer angles of the dark field detector. The scale bar is 0.5 nm. Intensity profile along the direction marked in (b) for (c) 5.8 nm, (d) 10.4 nm, and (e) 23.2 nm thick supercells. The intensity ratio of two columns with half the number of Ni atoms is 0.32, 0.41, and 0.48 respectively. The intensity ratio increases as a function of thickness and becomes proportional to the number of Ni atoms at about 25 nm.

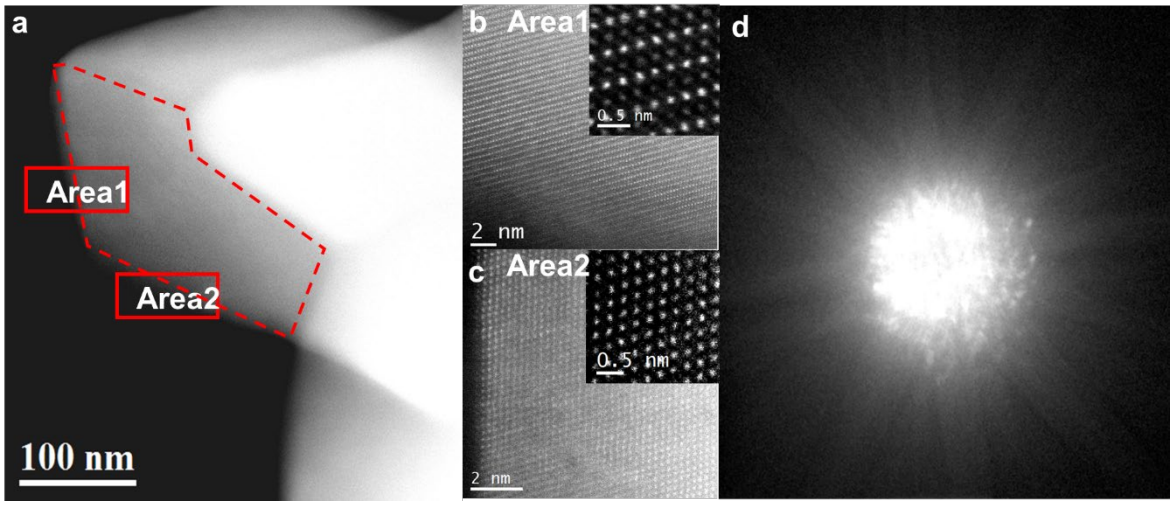

Figure S2: Presence of layered and rocksalt-type contrasts in a single particle. (a) The dashed region comprises two facets marked as area 1 and area 2 which shows two types of contrast. (b, c) The high magnification image of area 1 (rocksalt contrast) and area 2 (layered contrast). (d) The CBED pattern used to tilt this region along [110] layered is shown in d.

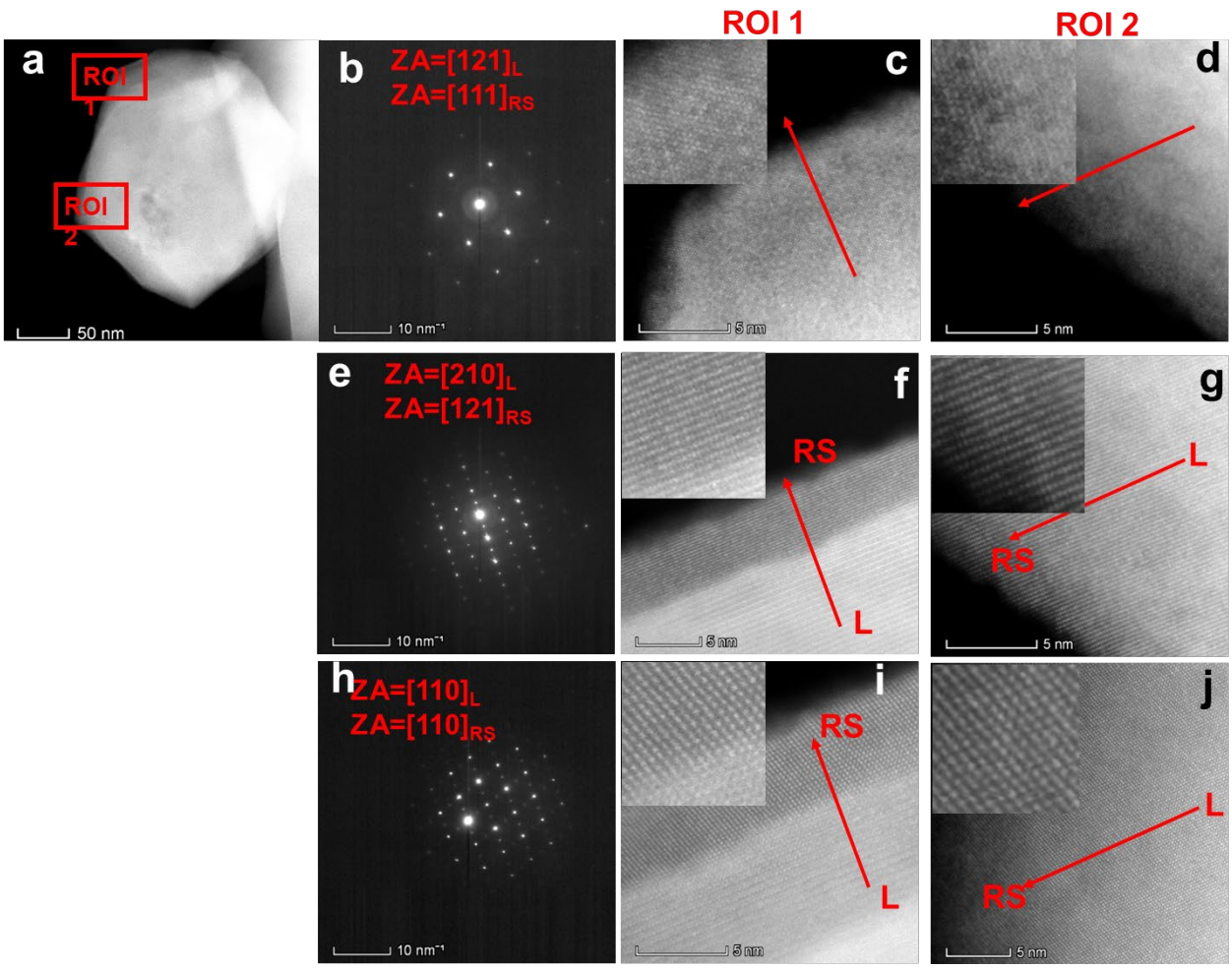

Figure S3: (a) Two transformed areas, ROI 1 and ROI 2 are tilted along [121], [210], and [110] zone axis directions with respect to the layered structure. (b-d) Along [121] direction the RS and layered contrasts are indistinguishable as the {003} reflections are not present along this direction. (e-j) Along the [210] and [110] directions, however, the RS and layered contrast are easily distinguishable. As we tilt the particle along the layered [121], [210], and [110] zone axis, the corresponding contrast changes in the RS area correspond to [111], [121], and [110] zone axis respectively of the cubic structure.

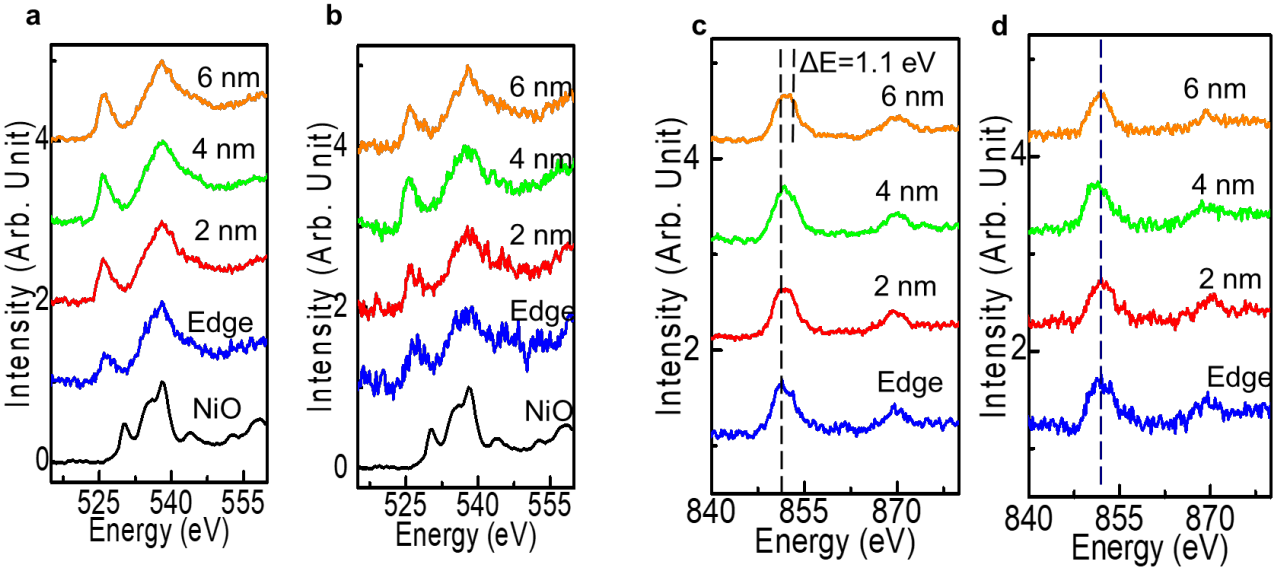

Figure S4: The core loss spectra as a function of distance in the area with (a,c) the layered and (b,d) RS contrast. Figures a, b depict O-K edge and figures c,d show the Ni-L edge. For O-K edge NiO spectrum is shown below as a reference. In case of figure c, there is shift in Ni-L edge indicating reduction at the surface.

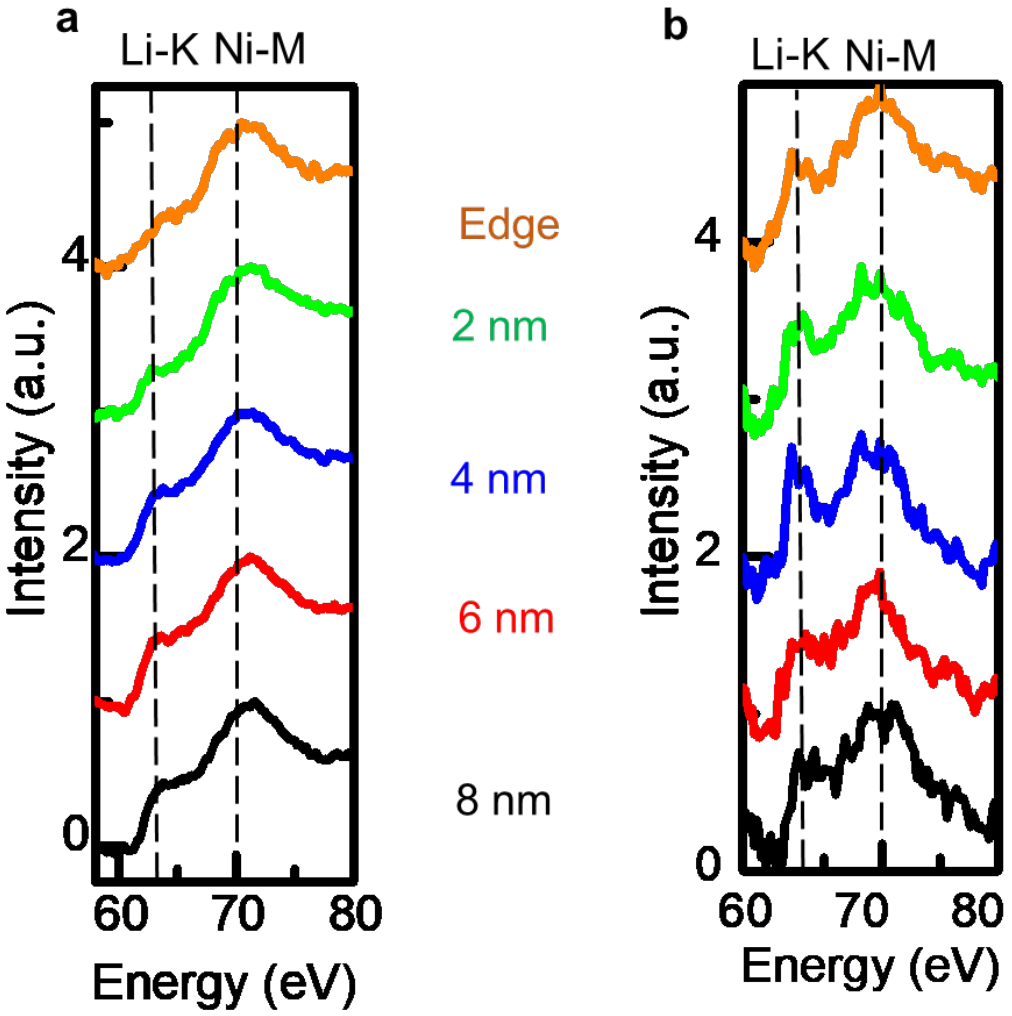

Figure S5: The low loss spectra as a function of distance in the area with (a) the layered and (b) RS contrast. The Li content is lower at the surface. In the "RS-like" area the intensity of Li(K) edge does not vary as a function of distance from the edge. In addition, the Li content appear the same or is higher than that in the layered structure.

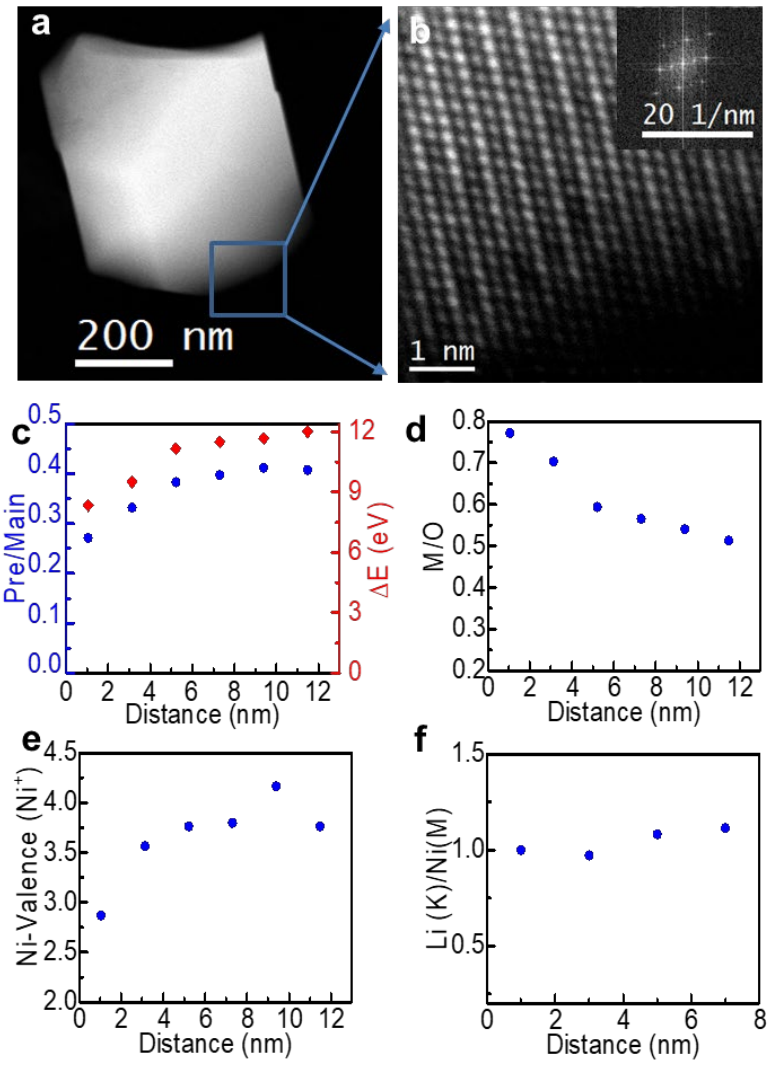

Figure S6: (a) ADF STEM image of NCA held at 4.5V for 2 weeks. (b) Magnified view of the surface and corresponding FFT. The contrast is layered-like ($R\bar{3}m$) with Ni atoms present in Li layer and corresponding EELS results as a function of distance with (c) Intensity ratio of O K-edge pre and main peaks and their difference. These values saturate around 10 nm from the edge. d) Ni valence increases from 2.6 to 3.7. (e) M/O ratio shows a decrease from 0.8 to about 0.5 indicating a reduced surface at the very edge of the particle (f) The Li(K)/Ni(M) ratio shows a small increase from 1.0 to 1.1.

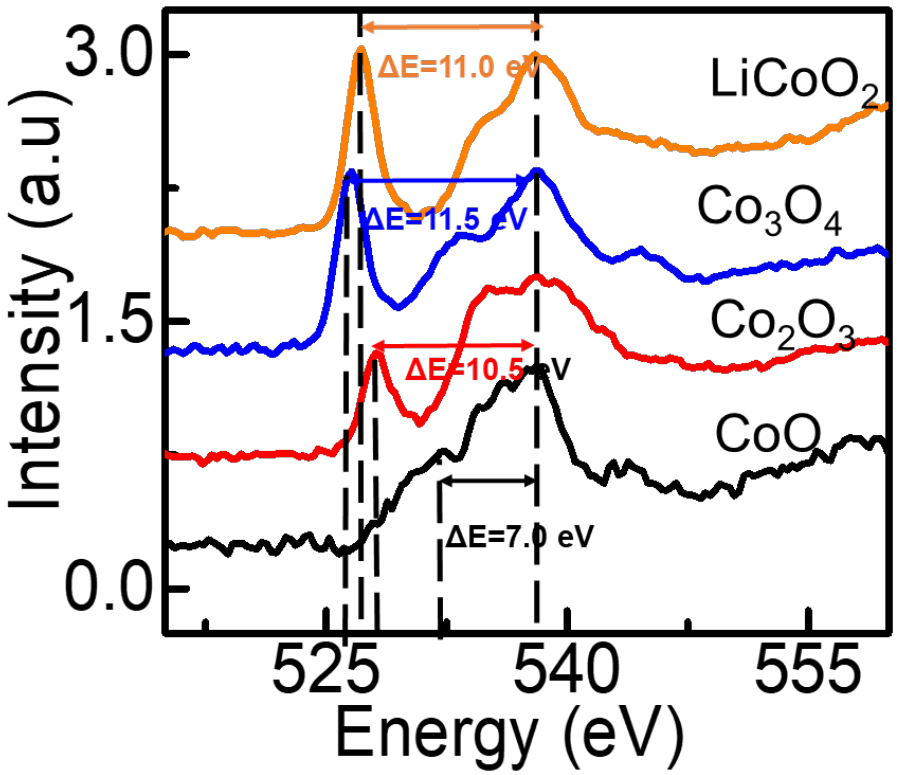

Figure S7: Characteristic EELS spectra of various cobalt oxides corresponding to layered ($R\bar{3}m$) $LiCoO_2$, spinel ($Fd\bar{3}m$) Co_3O_4, trigonal ($R\bar{3}c$) Co_2O_3 and rocksalt ($Fm\bar{3}m$) CoO. Spinel and layered structures have similar EELS characteristics.

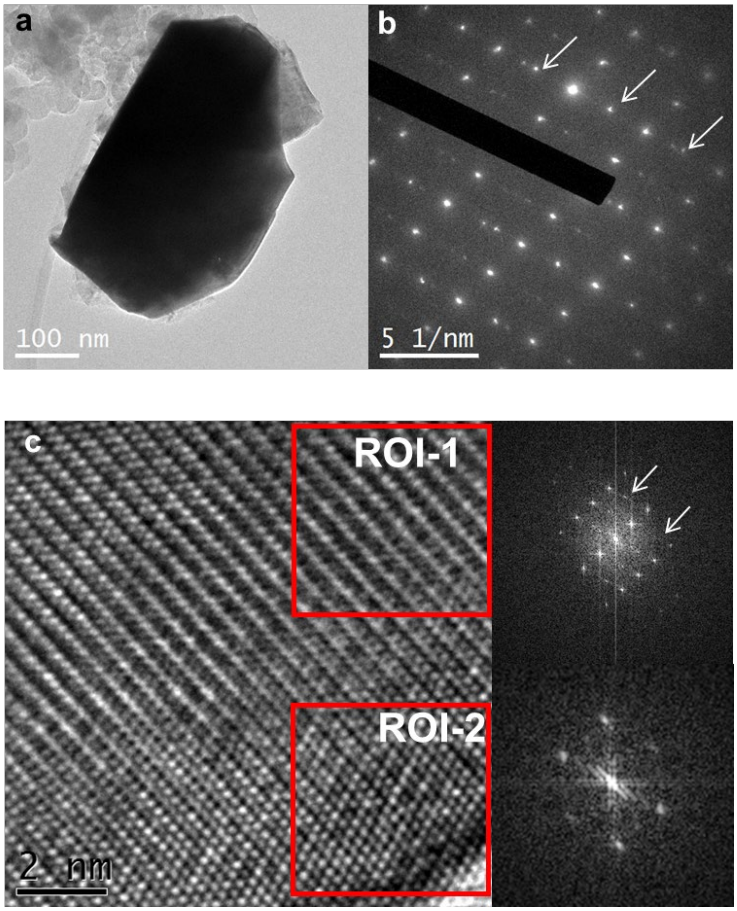

Figure S8: (a) Low magnification HRTEM image of NCA after high temperature (60 ˚C) aging for 2 weeks at 4.5V. The square area is where diffraction and HRTEM measurements were taken. (b) The SAED diffraction pattern from the near surface region can be indexed as the spinel ($Fd\bar{3}m$) structure. The arrows mark the additional reflections from layered $R\bar{3}m$. (c) HRTEM image with corresponding FFT patterns from area marked 1 and 2. Region 1 shows spinel-like contrast with additional spots in the FFT pattern marked by arrows similar to the SAED pattern. In region 2, reflections corresponding to $Fm^{-}3m$ rocksalt are observed.

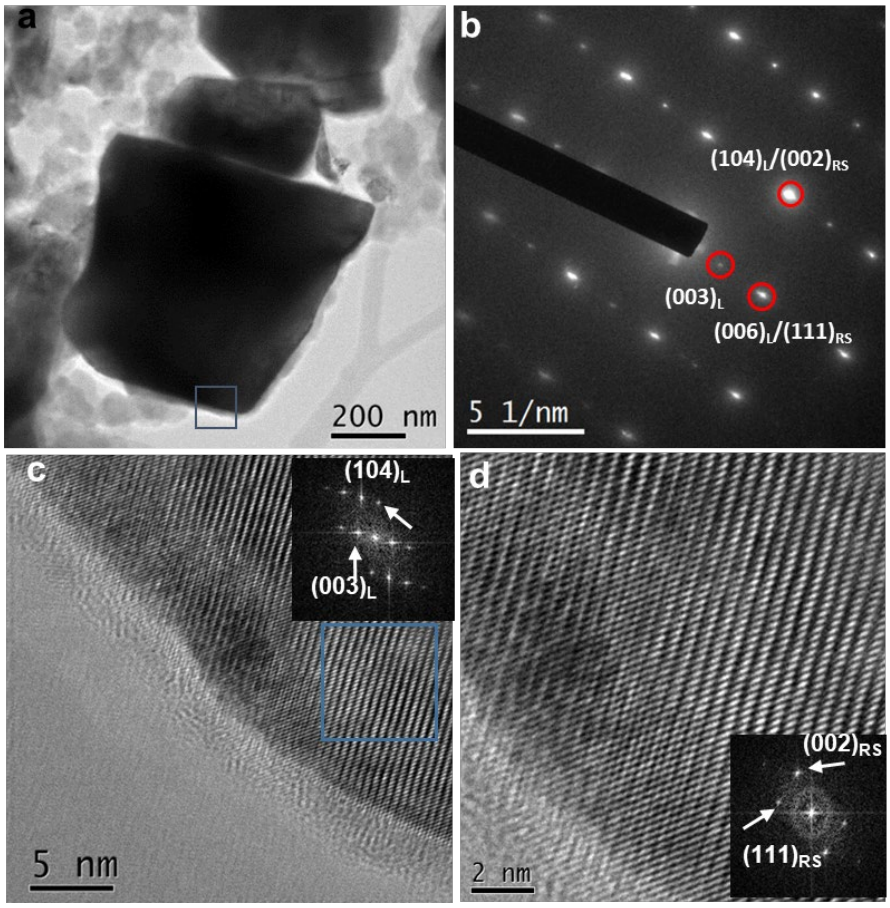

Figure S9: (a) Low magnification HRTEM image of NCA after high temperature (60 ˚C) aging for 10 hours at 4.75V. The square area is where diffraction and HRTEM measurements were taken. (b) Diffraction pattern from the near surface region which is indexed as the superposition of ($R\bar{3}m$) layered structure with ($Fm\bar{3}m$) rocksalt structure. The presence of rock salt structure is deduced from the alternative weak-strong reflections in the pattern with the strongest spots belonging to the rocksalt phase. (c) HRTEM image and corresponding FFT at the sub-surface show a layered ($R\bar{3}m$) phase and (d) enlarged HRTEM of the surface with corresponding FFT showing ($Fm\bar{3}m$) rocksalt type contrast.

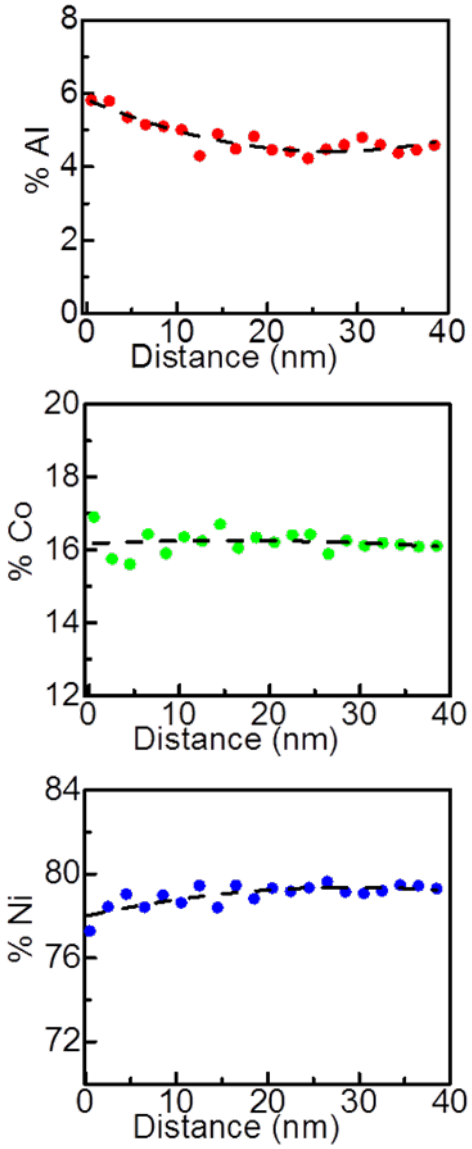

Figure S10: X-Ray EDS concentration profile of pristine NCA showing concentration profile (at.%) of (a) Al, (b) Ni and (c) Co revealing an Al enrichment at the surface from 4.5 to 6%.

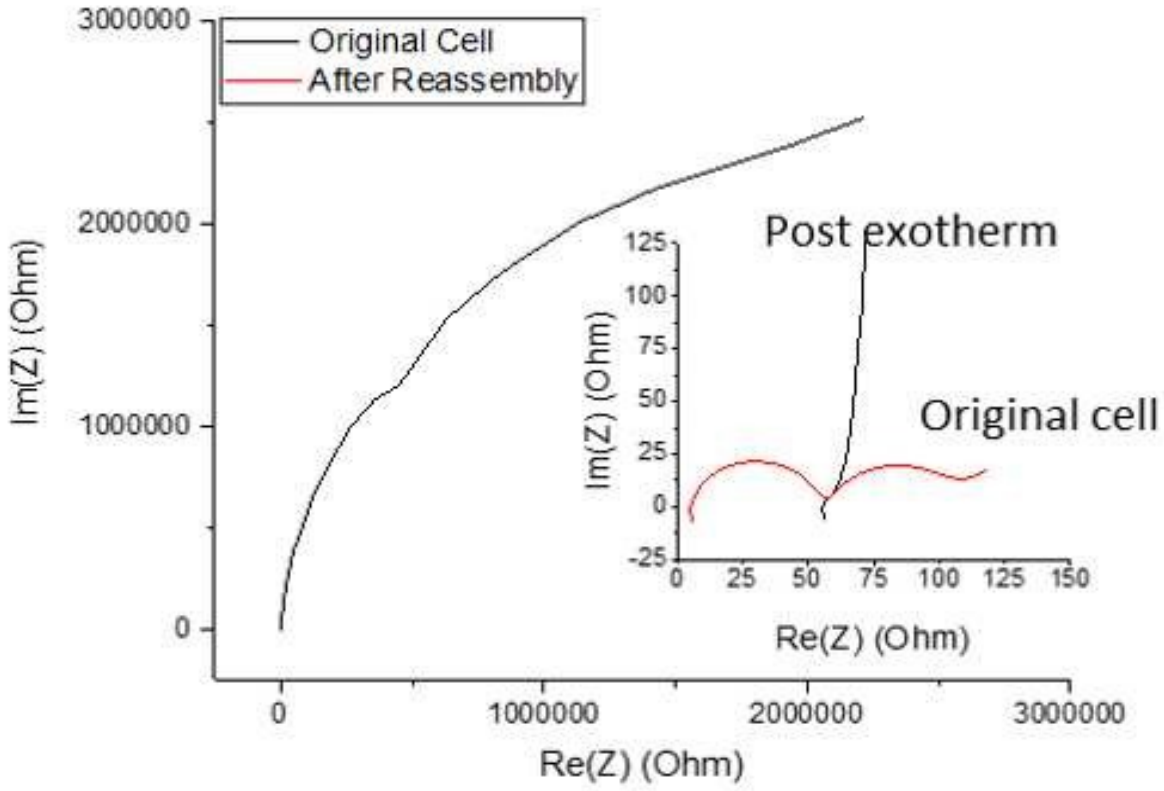

Figure S11: Impedance measurement of NCA after the exothermic reaction at 4.75V and 60 ˚C. A very large rise in impedance rise has been observed at this condition which is due to transition metal cation (Ni^{+2}, Co^{+2}) dissolution and plating on to the anode. The impedance drops sharply after the anode is substituted with a new one indicating that the large impedance rise can be attributed to the anode.

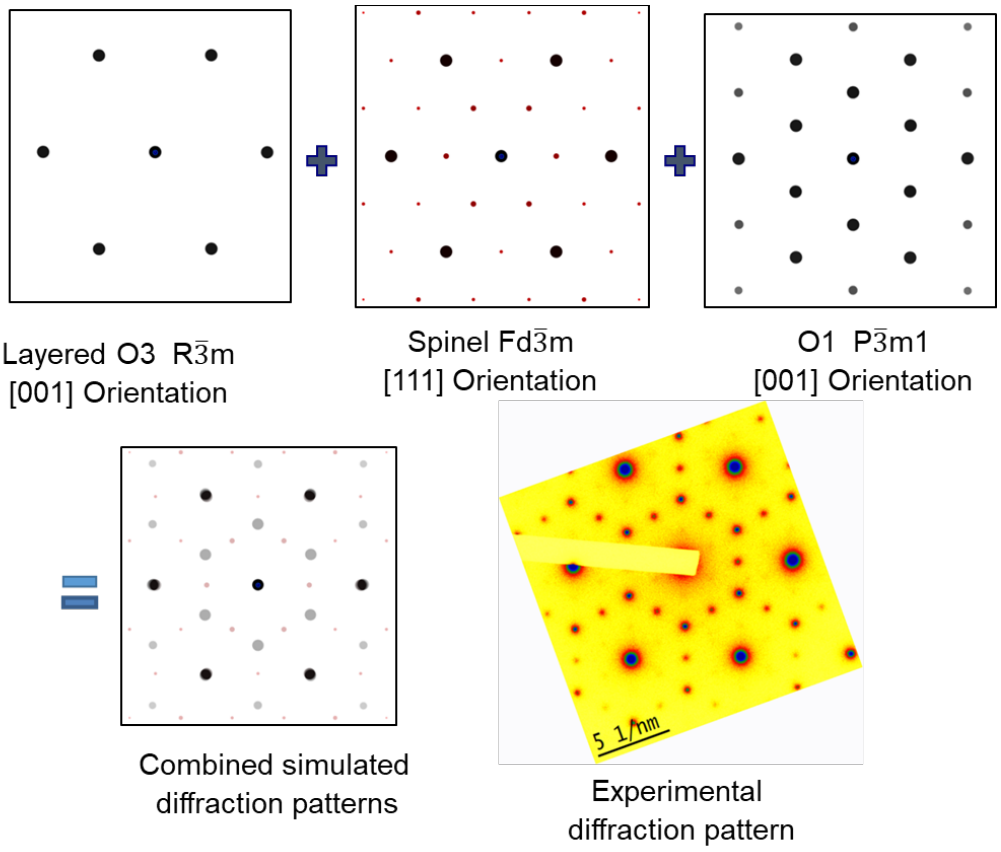

Figure S12: Simulated and experimental electron diffraction patterns of NCA held at 4.75 V and at 60 °C for 120 hours. The diffraction pattern can be indexed as the superposition of three phases with topotactic relationship corresponding to O3 (R$\bar{3}$m) ZA [001], spinel (Fd$\bar{3}$m) ZA [111], and O1 (P$\bar{3}$m1) ZA [001]. In the experimental SAED pattern, the very weak spots close to the transmitted beam are from double diffraction.